Proceedings of 34nd International Conference on Offshore Mechanics and Arctic Engineering
OMAE'15
May 31-June 5 , 2015, St.John's, Canada

OMAE2015-41961

NUMERICAL STUDY OF BILGE-KEEL EFFECT ON PARAMETRIC ROLL AND WATER ON DECK FOR AN FPSO

Marilena Greco
Centre for Autonomous Marine Operations and Systems (AMOS), Department of Marine Technology, NTNU, Trondheim, Norway.
CNR-INSEAN, Rome, Italy.
Email: marilena.greco@ntnu.no;marilena.greco@cnr.it

Claudio Lugni
CNR-INSEAN, Rome, Italy.
Centre for Autonomous Marine Operations and Systems (AMOS), Department of Marine Technology, NTNU, Trondheim, Norway.
Email: claudio.lugni@cnr.it

Giuseppina Colicchio
CNR-INSEAN, Rome, Italy.
Centre for Autonomous Marine Operations and Systems (AMOS), Department of Marine Technology, NTNU, Trondheim, Norway.
Email: giuseppina.colicchio@cnr.it

Odd M. Faltinsen
Centre for Autonomous Marine Operations and Systems (AMOS), Department of Marine Technology, NTNU, Trondheim, Norway.
Email: odd.faltinsen@ntnu.no

ABSTRACT

This research activity represents the logical continuation of the work documented in [1] and [2] on water on deck and parametric roll for an FPSO in regular waves. Here the same numerical method, based on a domain-decomposition strategy, is used to examine the platform with bilge keels, both without and with mooring-line system. It is found that bilge keels with length 40% of the ship length and with breadth the 3% of the ship breadth limit effectively the roll when instability is promoted by vertical bow motions in waves. In these conditions also the amount of the shipped water is substantially reduced. Large roll induced by the coupling with the lateral motions seems to be less well counteracted and remains close to 10° for steepness $kA \geq 0.2$. This value is often set as maximum allowed amplitude for FPSOs in normal operational conditions. Also the effect on the shipped water is limited in this case. Increasing the bilge-keels breadth is confirmed to be beneficial but the combination of the mooring system with dynamic positioning appears needed for a proper control of the roll motion in the worst examined cases.

INTRODUCTION

Weather-vaning FPSOs are mostly exposed to head-sea waves and can be subjected to water-on-deck (WOD) events, depending on the incident systems, while parametric roll (PR) is not recognized as a danger for such ships. Parametric roll is known as a resonance and instability phenomenon of the roll motion due to the fact that relative vertical ship motions cause variations of the transverse metacentric height connected with changes of the waterplane area and of the vertical position of the center of buoyancy relative to the center of mass. A clear explanation of the phenomenon and the critical conditions for its occurrence can be found, for instance, in [3] and along the years many studies have been carried out on the instability conditions and features by trying to account for the coupling of roll with heave and pitch motions in the time evolution of the restoring moment (see *e.g.* the review in [4] and very recent work in [5]).

The present research activity examines numerically the occurrence and features of parametric roll and water on deck on an FPSO interacting with regular waves. The analysis is the logical continuation of the two research investigations presented in [1]

and [2]. In [1], an inconvenience in the experimental set-up of an FPSO model highlighted occurrence of parametric-roll events promoted by yaw-roll coupling. The platform was without bilge keels and mooring lines and was examined in head- and bow-sea regular waves in the zone of the first parametric resonance. A combined physical and numerical analysis was then carried out on the relevance of this phenomenon on the roll resonance, as well as on the water shipping. Numerically, a 3D Domain-Decomposition (DD) strategy was adopted, combining a weakly-nonlinear potential-flow solver based on the weak-scatterer theory with a shallow-water approximation for the shipped water. In [2], the numerical solver was extended to model the loads due to mooring lines and PR and WOD were investigated for the same FPSO assumed with a turret single-point mooring-line system. From the results, sway and yaw tend to bring the system into an unstable regime with chaotic features.

Here the same numerical method is used to investigate the same FPSO equipped with bilge keels so to assess their relevance in improving the platform behavior in waves, both without and with mooring-line system. In the next section the numerical method is briefly outlined. Then the data of the FPSO are provided, together with the information of the model tests and findings from previous physical and numerical studies relevant for the present parameter investigation. The latter is presented both for the case without and with mooring-line system and then the main conclusions are drawn.

THE NUMERICAL SOLVER

The numerical solver consists of a Domain-Decomposition (DD) strategy and has been detailed documented in previous works, see *e.g.* [6] for the basic formulation and [2] for the method including the mooring-line modelling. Here the main features relevant for the physical investigation are recalled.

The method examines the problem of a 6-dof ship without or with a small forward speed and interacting with incident, regular or irregular, waves. The seakeeping potential-flow problem is handled within the weak-scatterer hypothesis (see *e.g.* [7]), which assumes the incident waves and body motions large with respect to the scattering and radiation waves and so it is valid for wavelength-to-ship length ratio sufficiently large. The impermeability body-boundary condition is satisfied averagely along the instantaneous wetted hull surface defined by the incident waves and the body motions, leading to a correction of the linear scattering and radiation loads. Nonlinearities are retained up to the second order for Froude-Krylov and hydrostatic loads. The method can handle bottom slamming by mean of a local velocity-pressure criterion combined with a Wagner-type solution. Here this modelling is not used because such phenomenon is not relevant in the present study. Occurrence of water shipping in the bow area is checked examining the local relative vertical motion between the waves (incident, scattering and radiation waves) and the vessel along the deck profile and then assessing the water tendency to invade the deck by means of the incident-wave velocity component normal to the deck profile (and in the plane of the deck) relative to the ship. Its induced local loads are estimated within a nonlinear shallow-water approximation, which is suitable to describe the global features of the most common type of water-on-deck scenario involving a dam-breaking type flow. The mooring-line system is modelled as a set of steel inelastic anchor-lines attached to the ship through a turret and radially distributed. All cables have the same pretension T_0 and the same total length. The horizontal tension, $T_{h,i}$, induced by each cable i on the vessel as a consequence of the action and reaction principle is obtained assuming a quasi-static approach but retaining a nonlinear cable description consistently with the approach indicated as method 2 in [8]. Once estimated all $T_{h,i}$ and known the instantaneous configuration of the cables, the surge and sway force and the yaw moment induced by the whole mooring system on the ship can be estimated at the examined time instant.

The DD solver estimates only the wave-radiation potential-flow damping. Other damping contributions can be modelled introducing additional damping terms, based on empirical formulas, in the equations of motion. In particular for the FPSO analyzed in this paper, the viscous roll damping for the vessel without bilge-keels and mooring-line system has been identified from free-decay tests and well modelled as a linear damping load with a damping coefficient B_{44h} equal to the 2.62% of the critical damping. The roll bilge-keel damping is modelled using the simplified formula in [9] obtained as best-fitting of the Ikeda's method. In this case, the nondimensional equivalent-linear damping coefficient is a function of many nondimensional parameters, in particular

$$\frac{B_{44bk}}{\rho\nabla B^2}\sqrt{\frac{B}{2g}} = f(\frac{B}{D}, C_b, C_m, \frac{OG}{D}, \omega\sqrt{\frac{B}{2g}}, \xi_{4,a}, \frac{b_{bk}}{B}, \frac{l_{bk}}{L}) \qquad (1)$$

with ρ the water density, ∇ the displacement, B the ship beam, D the ship draft, C_b the block coefficient, C_m the mid-ship coefficient, OG the vertical position of the center of gravity relative the calm-water free surface (positive downwards), ω the circular frequency, $\xi_{4,a}$ the roll amplitude, l_{bk} the bilge-keel length and b_{bk} the bilge-keel width. This formula is convenient with respect to the direct use of the Ikeda's method because the involved parameters are limited to general ship features and main bilge-keel dimensions. This fits well the purpose of this analysis which does not pretend to go in the details of a bilge-keel design but to apply an overall measure of their effect from hydrodynamic point of view, *i.e.* in terms of roll-damping moment. This damping modeling could be conservative for FPSOs, especially with large bilge-keels. In this case de Oliveira *et al.* [10] observed that a damping saturation can occur for sufficiently large roll angles. The mooring-line damping loads for surge (1) , sway (2) and yaw (6) are assumed as velocity-square damping terms with

coefficients corresponding to equivalent linear coefficients equal to $0.1B_{jjcr}\omega\xi_{ja}8/(3\pi)$, with j = 1,2 and 6, and B_{jjcr} and ξ_{ja} the critical damping and motion amplitude, respectively. With this choice the transient stage is practically not affected by such damping, typically small. A more in-depth investigation for a better modelling of these damping contributions is left for a future work while the present activity focuses on the influence of the bilge-keel damping.

The different loads are inserted in the rigid-body motion equations written along a body-fixed coordinate system with origin in the center of gravity and following the approach in [11]. They read

$$M\ddot{\xi} + \Omega \times M\dot{\xi} + A_\infty\dot{\beta} + \int_0^t K(t-\tau)\dot{\beta}(\tau)\,d\tau = F_{0\,\mathrm{nlin}} + F_{h\,\mathrm{nlin}} + F_{\mathrm{wod}} + F_{\mathrm{moor}} + F_{\mathrm{add}}\,. \quad (2)$$

Here, M is the ship generalized mass matrix, $\xi \equiv (\xi_1,..,\xi_6)$ are the six rigid degrees of freedom, Ω is the angular velocity vector $(\dot{\xi}_4,\dot{\xi}_5,\dot{\xi}_6)$ with components along the instantaneous body axes and the upper dots indicate time (t) derivatives. Further, A_∞ is the infinite-frequency added-mass matrix, K is the retardation function matrix and the components of β are obtained enforcing the instantaneous impermeability condition within the weak-scatterer assumption (see *e.g.* [7]). In the left-hand side of the motion equations, the second term is the inertial-load contribution due to the body-fixed coordinate system and the third and fourth terms correspond to radiation and scattering loads which are combined within the weak-scatterer hypothesis. In the right-hand side, we find the nonlinear loads due to water-on-deck (F_{wod}), mooring-line system (F_{moor}), Froude-Krylov ($F_{0\,\mathrm{nlin}}$) and hydrostatic ($F_{h\,\mathrm{nlin}}$) contributions. Finally the last term (F_{add}) accounts for additional linear or square-velocity damping contributions.

The equations of motions are solved in time using a fourth-order Runge-Kutta scheme. When evolving from time t to $t+\Delta t$ the water-on-deck loads, the convolution-integral terms and the mooring-line loads are estimated in t and retained constant during the interval Δt, while the remaining loads are estimated at any time instant required by the scheme.

FPSO PLATFORM AND PREVIOUS STUDIES

The main information of the selected FPSO is given in table 1. Previous studies on this platform, without and with mooring lines, are summarized in the following. Experimental data and same operational conditions are used in the next section to carry on a numerical investigation on the influence of bilge-keels on the occurrence and features of ship instability and water shipping.

FPSO without mooring-lines This vessel was studied experimentally at the CNR-INSEAN basin no. 2 (length x width x depth = 220 x 9 x 3.6 m) in scale 1:40 without bilge keels and mooring-line systems. Detailed discussion of the tests, of the performed measurements and of the accuracy, can be found in [2] and [1]. The model tests were targeted to examine water-on-deck and parametric-roll phenomena in regular waves in head-sea ($\alpha = 180^\circ$) and two bow-sea ($\alpha = 175$ and 170°) conditions. They are provided in tables 2-5 in terms of the steepness kA, with k the wavenumber and A the wave amplitude and in terms of the calm-water roll natural frequency-to-prescribed excitation frequency ratio ω_{4n0}/ω for PR while the corresponding prescribed wavelength-to-ship length ratio λ/L is used for WOD. This is done because ω_{4n0}/ω is a relevant parameter for the PR occurrence while λ/L is important when examining the WOD occurrence. In particular, the chosen ω_{4n0}/ω range indicates that the waves are in the region of first parametric resonance for the roll and the corresponding λ/L range is in the region of heave and pitch resonance. One must note that due to some problems with the wavemaker, there were some differences between prescribed and realized waves. Here the prescribed quantities are provided, the actual incident waves parameters are documented in [1]. The experiments were designed to restrain surge, sway and yaw by means of a gimble placed in the hull combined with a vertical shaft. In reality, during the tests the yaw motion was not properly restrained because of a slack in the shaft. The involved amplitudes were negligible in head-sea conditions and with $\alpha = 175^\circ$ until the case with $\omega_{4n0}/\omega = 0.519$ and $kA = 0.25$ was tested as run 44. This incident wave did not cause PR but induced severe WOD with profound leakage of water inside the model. As a result, the shaft slack worsened. When the test was repeated as run 46 the yaw motion was not negligible and both PR and

TABLE 1. MAIN PARTICULARS OF THE FPSO AT FULL SCALE.

Length ($L = L_{pp}$)	168.8 m
Breadth (B)	32.4 m
Draft (D)	10.0 m
Freeboard (f)	9.9 m
Displacement(∇)	43493 t
Block coefficient (C_b)	0.77
Mid-ship coefficient (C_m)	0.99
Height of center of gravity (KG)	0.71D
$OG = KG - D$	-0.29D
Roll Gyration radius	0.37 B
Pitch Gyration radius	0.27 L
Yaw Gyration radius	0.27 L
Transverse metacentric height (GM)	1.44 m

WOD were caused. The combined physical and numerical investigation, using the method described in the previous section and documented in [1], highlighted the crucial role of the yaw-roll coupling for the roll instability in this case and for the tuning of the roll natural period to $1.5T$ instead of $2T$ as usual for the first parametric resonance, T being the incident-wave period. From the analysis, the amplitude of the resonant roll is affected by the coupling with the other degrees of freedom. In particular, the coupling with yaw, experienced by the ship in bow-sea waves, can cause roll instability and tends to increase the steady-state roll amplitude and to reduce the roll natural period with respect to the case with restrained yaw. The first parametric resonance promoted by coupling with heave and pitch motions is characterized by the tuning of the roll natural period to $2T$, with T the excitation period. The coupling with yaw leads to a tuning of the yaw natural period to $3T$ and moves the tuning for the roll to $1.5T$. It also affects the water shipping. The trend is in reducing the phenomenon severity for the vessel in the examined incident waves. This is opposite to the influence of the parametric roll on the water on deck in head-sea waves and zero yaw, as documented in [12].

FPSO with mooring-lines In order to investigate the importance of motions coupling in the excitation of roll instability, the FPSO was modelled numerically as moored in a water region with depth 200 m by assuming a mooring-line system as used in practice. In particular, ten mooring-lines, each with total length about 1584 m, were distributed radially at $72 \times i \pm 2.5$ degrees (i=0,1,2,3,4) from the platform longitudinal axis with basic configuration involving a turret longitudinal position at $0.25L$ ahead of mid-ship and a pretension $T_0 = 2000$ kN. A systematic analysis was then performed by varying incident wavelength, steepness, heading, location of the turret and pretension. From the analysis, sway and yaw tend to destabilize the system also exciting chaotic features. The sway-roll-yaw coupling promotes the PR resonance and leads to larger amount of shipped water, especially at smaller wavelength-to-ship length ratio and larger steepness. The chaotic features appear to be excited when a sufficiently large yaw amplitude is reached, suggesting an important role of nonlinear effects for the stability regime. The mooring-line system leads to small restoring and so to large natural periods for the horizontal motions. As a consequence, the sway-roll-yaw coupling is not able to modify the roll natural period when PR occurs, as instead documented by the experiments with shaft slack. However the roll experiences a chaotic behavior, associated to the amplitude, due to the coupling with sway and yaw. It was also confirmed that the horizontal motions can be successfully controlled and their induced instability avoided when a suitable dynamic-positioning (DP) system is combined with the mooring lines. Further investigations should account for state-of-the-art second order excitation slow-drift oscillations.

PHYSICAL INVESTIGATION

Here, the effect of the bilge-keel damping is investigated in both FPSO conditions described in the previous section. The required ship parameters for formula (1) can be found in table 1 and are within the range of validity of the simplified formula. The roll amplitude is calculated run-time during the simulation so to account for transient conditions. Finally the bilge-keel dimensions are needed and, for the formula validity, they should be so that $0.01 \leq b_{bk}/B \leq 0.06$ and $0.05 \leq l_{bk}/L \leq 0.4$. Here they are assumed $b_{bk} = 0.03B$ and $l_{bk} = 0.4L$. For the breadth this corresponds to about 1 m at full scale. Typically, for FPSOs it is used a breadth between 0.8 to 1 m and in some cases up to 1.4m. For the length it was chosen the upper limit of the formula applicability though, for FPSOs, l_{bk}/L could be 0.5 and in some case up to 0.7.

Unless explicitly stated, all examined numerical simulations are performed for $400T$ with a time step Δt=$0.005T$ and the water shipping is solved on a squared Cartesian grid in the deck plane with mesh size $\simeq 0.0008L$.

FPSO without mooring-lines Parametric-roll occurrence at $\alpha = 180^\circ$ and 175° is analyzed in tables 2 and 3 providing the roll amplitude in case of PR. In these and in tables 4 and 5 the symbol 'X' indicates cases not studied experimentally. Excluding the cases of PR connected with the yaw-roll coupling due to the shaft slack, there is not much difference in terms of instability occurrence at the two headings and also the amplitudes involved are similar. Moreover the PR is supported by larger kA at $\omega_{4n0}/\omega = 0.402$ and counteracted at $\omega_{4n0}/\omega = 0.464$. The solver without bilge-keel damping and zero yaw is in good agreement with the model tests in terms of occurrence of PR, but there

TABLE 2. $\alpha = 180^\circ$: EXPERIMENTAL AND NUMERICAL OCCURRENCE OF PARAMETRIC ROLL (PR) WITHOUT (W/O) AND WITH BILGE-KEELS. ROLL AMPLITUDES ARE IN DEGREES.

$\omega_{4n0}/\omega \rightarrow$	0.402	0.464	0.519	0.568	0.656
Method kA			PR		
Exp. 0.10	NO	21.3±0.3	NO	NO	NO
w/o 0.10	NO	19.3/16.2	NO	NO	NO
with 0.10		2.6			
Exp. 0.15	NO	15.4±0.3	NO	NO	NO
w/o 0.15	NO	13.2	NO	NO	NO
with 0.15		3.9			
Exp. 0.20	26.7±0.4	NO	NO	NO	X
w/o 0.20	24.6	8.4	NO	NO	X
with 0.20	$<< 1.0$	$<< 1.0$			
Exp. 0.25	27.2±0.4	NO	NO	NO	X
w/o 0.25	23.1	NO	NO	NO	X
with 0.25	3.2				

TABLE 3. $\alpha = 175^\circ$: EXPERIMENTAL AND NUMERICAL OCCURRENCE OF PARAMETRIC ROLL (PR) WITHOUT (W/O) AND WITH BILGE-KEELS. ROLL AMPLITUDES ARE IN DEGREES.

$\omega_{4n0}/\omega \rightarrow$	0.402	0.464	0.519	0.568	0.656
Method kA			PR		
Exp. 0.10	NO	17.9±1.7	NO	NO	NO
w/o 0.10	NO	15.9	NO	NO	NO
with 0.10		3.1			
Exp. 0.15	NO	16.4±1.3	NO	NO	NO
w/o 0.15	NO	11.3	NO	NO	NO
with 0.15		1.7			
Exp. 0.20	26.3±0.4	9.5±2.0	NO	11.3±3.7	X
w/o 0.20	25.0	6.3	NO	NO	X
with 0.20	2.6	NO			
Exp. 0.25	25.3±1.6	NO	NO/12.1±3.7	12.9±2.08	X
w/o 0.25	21.8	NO	NO	NO	X
with 0.25	3.0				

is not predicted any roll instability for the cases at $\alpha = 175^\circ$ with substantial shaft slack ($\omega_{4n0}/\omega \geq 0.519$). Also the involved amplitudes are close to the measurements with values in general quite large. More in detail, the numerics slightly underestimates the steady-state roll amplitudes recorded experimentally. On the numerical side, besides the limitations connected with the method assumptions, an error source is associated with the use of a linear roll damping estimated from the free-decay test in calm water with initial roll amplitude of about 11 degrees. In reality the damping can change both because of larger roll amplitudes involved and because the roll natural frequency can be modified by coupling with other motions and by nonlinear effects in the roll restoring moment. On the experimental side, an error source is connected with the presence of side walls affecting the roll motion in bow sea and in case of a misalignment of the ship in head sea. For incident waves with $\omega_{4n0}/\omega = 0.464$ and $kA = 0.1$ experimentally PR did not reach the steady-state conditions during the recorded time history, so the maximum roll amplitude is provided. This is also reported for the numerics, while the second numerical prediction for this case corresponds to the steady-state PR amplitude. The numerical cases with PR occurrence were repeated including the bilge-keel damping. This limits the PR amplitudes below 4° and avoids the instability completely for one case.

The occurrence of WOD for the cases discussed is provided in tables 4 and 5. There, 'NI' for the experiments means that the water shipping was observed but not periodically and was small. For the cases with water on deck, the tables give the maximum numerical amount of shipped water Q in steady-state conditions. This quantity was not measured in the experiments because the required arrangement would be complicated and could interfere with the vessel behaviour. So only videos of the water shipping were used to monitor the occurrence of the

TABLE 4. $\alpha = 180^\circ$: EXPERIMENTAL AND NUMERICAL OCCURRENCE OF WATER ON DECK (WOD) WITHOUT (W/O) AND WITH BILGE-KEELS. IT IS PROVIDED THE NUMERICAL MAXIMUM VOLUME OF SHIPPED WATER Q MADE NONDIMENSIONAL BY S_dA, WITH S_d THE DECK AREA.

$\lambda/L \rightarrow$	0.75	1.00	1.25	1.50	2.00
Method kA			WOD		
Exp. 0.10	NO	NO	NO	NO	NO
w/o 0.10	NO	NO	NO	NO	NO
with 0.10		NO			
Exp. 0.15	NO	NO	NI	NO	NO
w/o 0.15	NO	0.017	0.012	NO	NO
with 0.15		0.004			
Exp. 0.20	YES	YES	YES	YES	X
w/o 0.20	0.125	0.178	0.134	0.017	X
with 0.20	NO	0.177			
Exp. 0.25	YES	YES	YES	YES	X
w/o 0.25	0.190	0.507	0.356	0.055	X
with 0.25	0.036				

TABLE 5. $\alpha = 175^\circ$: EXPERIMENTAL AND NUMERICAL OCCURRENCE OF WATER ON DECK (WOD) WITHOUT (W/O) AND WITH BILGE-KEELS. IT IS PROVIDED THE NUMERICAL MAXIMUM VOLUME OF SHIPPED WATER Q MADE NONDIMENSIONAL BY S_dA, WITH S_d THE DECK AREA.

$\lambda/L \rightarrow$	0.75	1.00	1.25	1.50	2.00
Method kA			WOD		
Exp. 0.10	NO	NO	NO	NO	NO
w/o 0.10	NO	NO	NO	NO	NO
with 0.10		NO			
Exp. 0.15	NO	NI	NI	NI	NO
w/o 0.15	NO	0.052	0.042	0.003	NO
with 0.15		0.043			
Exp. 0.20	due to PR	YES	YES	YES	X
w/o 0.20	due to PR:0.162	0.262	0.151	0.030	X
with 0.20	NO	0.255			
Exp. 0.25	YES	YES	YES	YES	X
w/o 0.25	0.220	0.564	0.307	0.056	X
with 0.25	0.053				

events. Also in this case, the numerics without bilge-keel damping agrees well with the physical recordings of the water shipping. There are few cases where WOD is numerically predicted and either not recorded or not periodic and small experimentally. For these cases numerically the events were very limited in terms of amount of shipped water. From the numerics, the most severe WOD events occur at $\lambda/L = 1$ which is in the region of heave and pitch resonance. In this case larger relative vertical motions apparently occurred, leading to more pronounced freeboard exceedance. When the bilge-keel damping is introduced in the equations of motion the water shipping at $\lambda/L = 0.75$ and

$kA = 0.2$ is avoided. This is because the event is caused by the parametric roll which is practically killed by these appendages. It is interesting to note that the bilge keels are more effective in reducing Q at the lowest wavelength while their influence is limited at $\lambda/L = 1$. This suggests a limited role of PR on WOD at this wavelength, *i.e.* in this case the water shipping is dominated by heave and pitch and subsequent relative vertical motions.

Figure 1 examines the roll and yaw motion for run 46 when including the yaw in the simulations by means of an identification process from the measurements of the linearized restoring and damping coefficients connected with the yaw motion, as explained in *e.g.* [1] and [2]. The identification procedure has limited reliability for the damping coefficients so, in the research documented in the mentioned works, B_{46} (assumed equal to B_{64}) was initially set to the identified value and then reduced down to the sixty percent so to have numerical motion amplitudes more consistent with the experiments. Here, both B_{66} and B_{46} were varied so to achieve the best quantitative agreement with measured curves. Two conditions have been identified, referred to as case 1 and 2 in the figure. For both of them B_{46} is still the sixty percent of the identified value while B_{66} is, respectively, 2.2 and 2 times the identified value. These coefficients are given in terms of the yaw critical damping in the figure. As expected the two numerical results are associated with the same oscillation periods, consistent with the experiments. They are close to each other and to the measurements in terms of involved amplitudes while there is a phase shift and a small difference in mean value with respect to the physical yaw. On the other hand it is hard to reproduce with linearized restoring and damping loads the nonlinear effects caused by the shaft slack. For this case the yaw-roll coupling leads to a roll amplitude exceeding 15 degrees according to the experiments. The two numerical cases are associated with a roll amplitude around 17 degrees while the yaw amplitudes are about 5 and 4 degrees, respectively. Here the motion amplitude is defined as half of difference between the maximum

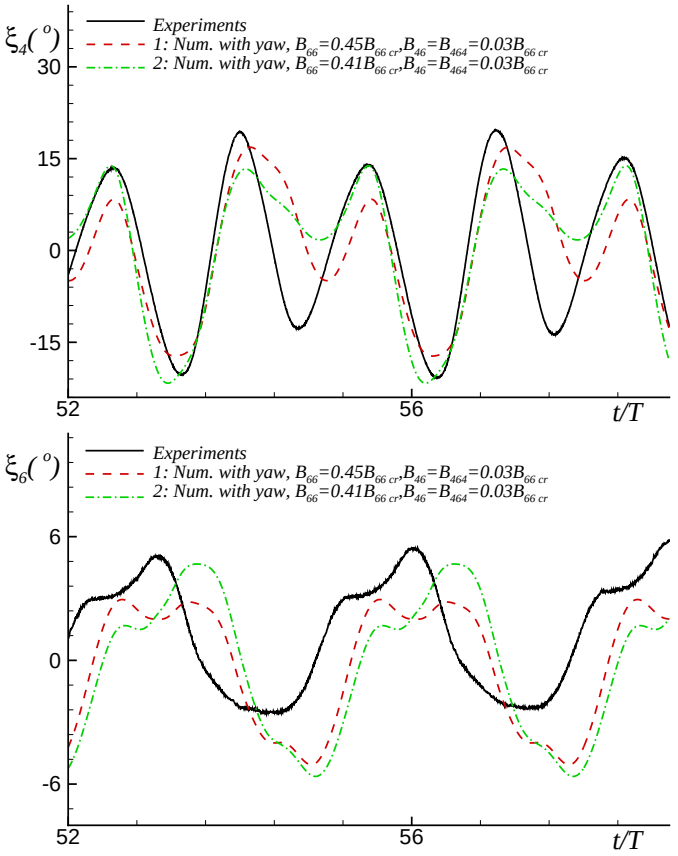

FIGURE 1. $\omega_{4n0}/\omega = 0.519$, $kA = 0.25$: ROLL (TOP) AND YAW (BOTTOM) FROM TEST 46 AND FROM THE DD SOLVER INCLUDING YAW MOTION AND WITHOUT BILGE KEELS.

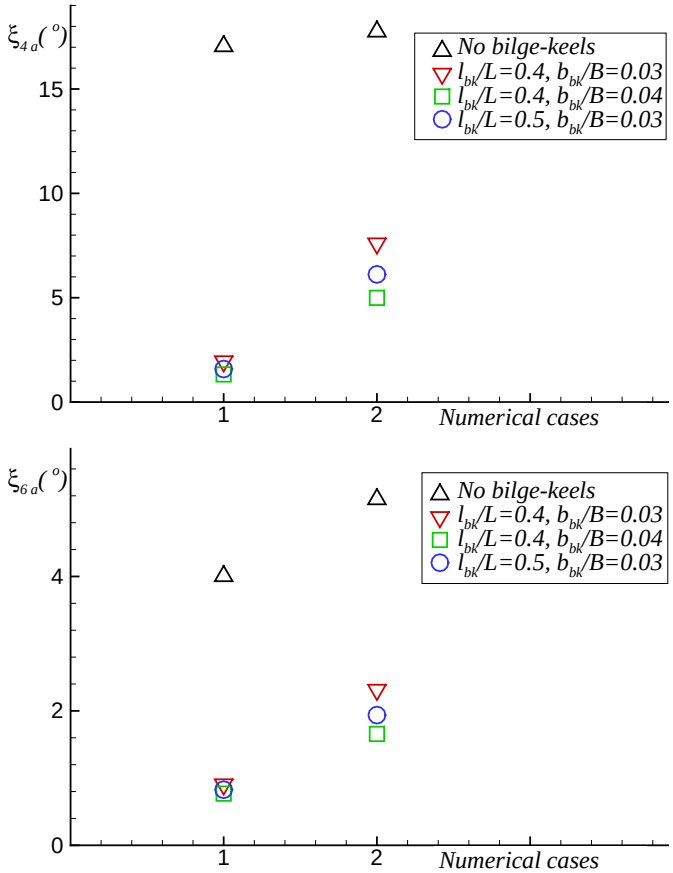

FIGURE 2. $\omega_{4n0}/\omega = 0.519$, $kA = 0.25$: NUMERICAL AMPLITUDE OF ROLL (TOP) AND YAW (BOTTOM) WITHOUT AND WITH BILGE-KEELS.

and minimum values after the initial transient. Despite the similar features shown by the two numerical cases, the bilge keels have a different effectiveness for the resulting systems, as shown in figure 2. In particular for case 1, the basic dimensions are suitable to limit the roll amplitude ξ_{4a} to about 2 degrees while for case 2 the same bilge-keels would be only able to keep it below 8 degrees. Due to the roll-yaw coupling, a similar trend is observed for the yaw amplitude ξ_{6a}. Assuming wider (b_{bk}/B=0.04, which is still of practical use) or longer (l_{bk}/L=0.5, it should be noted that this is out of the validity range for formula (1)) does not have much effect on the roll amplitude for case 1, probably because the additional damping in the roll is not able to further limit the yaw motion and so, in return, the roll amplitude. On the contrary, longer, but especially wider, bilge-keels can reduce the roll amplitude for case 2. In particular, with the chosen parameters ξ_{4a} goes down to about 5 degrees and ξ_{6a} to below 2 degrees. Figure 3 examines more in detail cases 1 and 2 without and with basic bilge-keels in terms of the time evolution of roll and yaw. Without the roll damping from these appendages, roll

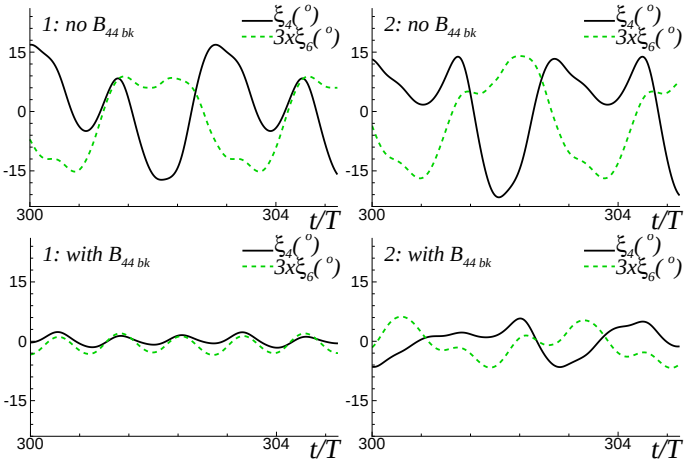

FIGURE 3. $\omega_{4n0}/\omega = 0.519$, $kA = 0.25$: NUMERICAL ROLL AND YAW WITHOUT AND WITH BILGE-KEELS (l_{bk}/L=0.4 AND b_{bk}/B=0.03) FOR CASE 1 AND 2 DEFINED IN FIGURE 1.

and yaw appear 180 degrees out-of-phase for most of the time during a yaw oscillation period. This is a bit more pronounced in case 2 for which the yaw damping coefficient B_{66} is slightly lower than for case 1. If ξ_4 is 180 degrees out-of-phase with respect to ξ_6, for instance, the cross-coupling moment $-B_{46}\dot{\xi}_6$ acts as a negative damping for the roll and similarly $-B_{64}\dot{\xi}_4$ acts as a negative damping for the yaw. This supports the instability. With the bilge-keel damping, for case 1 roll and yaw become in phase so that they tend to damp each others through their cross-coupling damping moments $-B_{46}\dot{\xi}_6$ and $-B_{64}\dot{\xi}_4$, and this is consistent with the much lower amplitudes of both motions. For case 2 instead, the two motions preserve out-of-phase features, likely because B_{66} is not large enough, and so they tend still to increase each other through the cross-coupling damping moments.

All the results suggest a primary role of yaw-roll coupling in exciting this instability behavior and the need of a proper lateral-motion control in conditions with free yaw. One must note that this analysis assumes that there is no effect of the bilge keels on B_{46} and B_{64}.

FPSO with mooring-lines The numerical study of the same FPSO in moored conditions and in same head-sea regular waves highlighted the importance of sway-roll-yaw coupling in destabilizing the system and bringing a chaotic behavior, as documented in [2].

Here the regular head-sea incident waves with $\lambda/L \in [0.75, 1.5]$ are considered because they appeared to be the most interesting for parametric roll of the vessel without mooring lines (see previous section) and the wave parameters are set as the actual waves from the experiments examined in the previous section. This is done so to allow also a comparison between the cases without and with mooring lines. More in detail, the actual head-sea waves in the model tests were consistent with the prescribed waves, but for case with $\lambda/L = 0.75$ and $kA = 0.2$ which was with $\lambda/L = 0.755$ and $kA = 0.21$ in reality. In the following, the relevant features of the instability phenomena due to the motions coupling are discussed. These are exemplified in the top plots of figures 4 and 5 examining $\omega_{4n0}/\omega = 0.464$ and, respectively, kA=0.15 and 0.2. The case with lower steepness is clearly characterized by parametric roll occurrence before excitation of sway and yaw motions (see enlarged view at smaller times in the top plot of figure 4) and so due to the influence in waves of the heave and pitch motions on the restoring moment. As time goes on the yaw motion shows oscillations with a period longer than the excitation period, reasonably connected with its natural period, and rises in amplitude with a clear instability behavior. The yaw brings into instability also the sway which follows a similar trend. Once the yaw has reached a sufficiently large value the maximum values of sway and yaw remain limited and randomly change in time and this leads to chaotic features also in the roll. The sway oscillations are dominated by a period about $24T$ which characterizes also the yaw evolution together with a lower period about $8T$. These large periods are not able to modify the roll natural period but promote a chaotic change of the roll amplitude. The roll is still dominated by its natural period which remains tuned to $2T$ as in a first parametric resonance (see enlarged view at larger time in the same plot). The bilge-keel damping is able to kill the roll amplitude connected with the initial PR phenomenon due to the heave and pitch motions and as a result also the later roll amplitudes appear more limited than without bilge keels, in particular below 8 degrees, but there is no effect of the reduced roll on the amplitudes of the horizontal motions (see bottom plot of figure 4). This confirms a dominant role of sway and yaw on this documented instability.

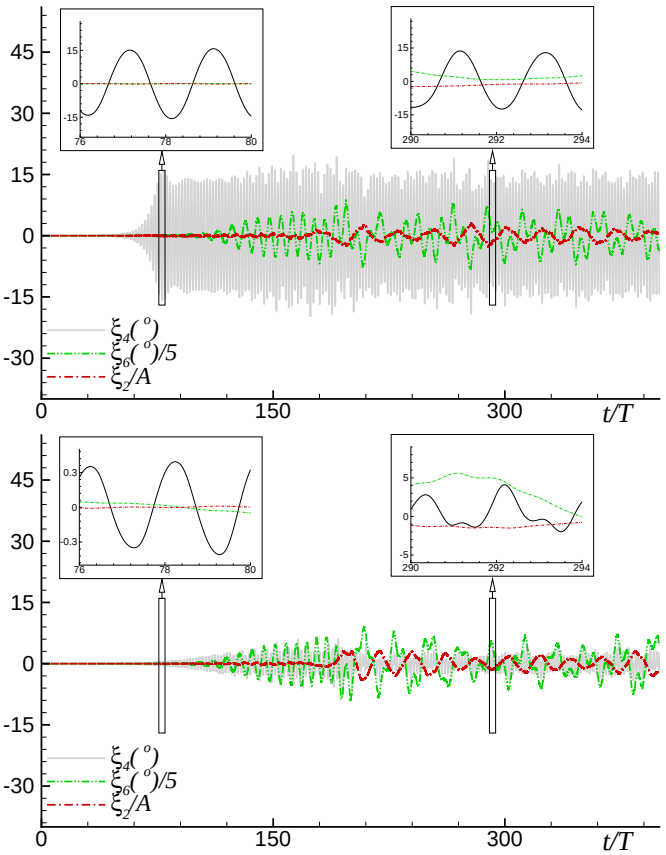

FIGURE 4. $\omega_{4n0}/\omega = 0.464$, $kA = 0.15$: NUMERICAL SWAY, ROLL AND YAW WITH MOORING-LINES, WITHOUT (TOP) AND WITH (BOTTOM) BILGE KEELS (l_{bk}/L=0.4 AND b_{bk}/B=0.03).

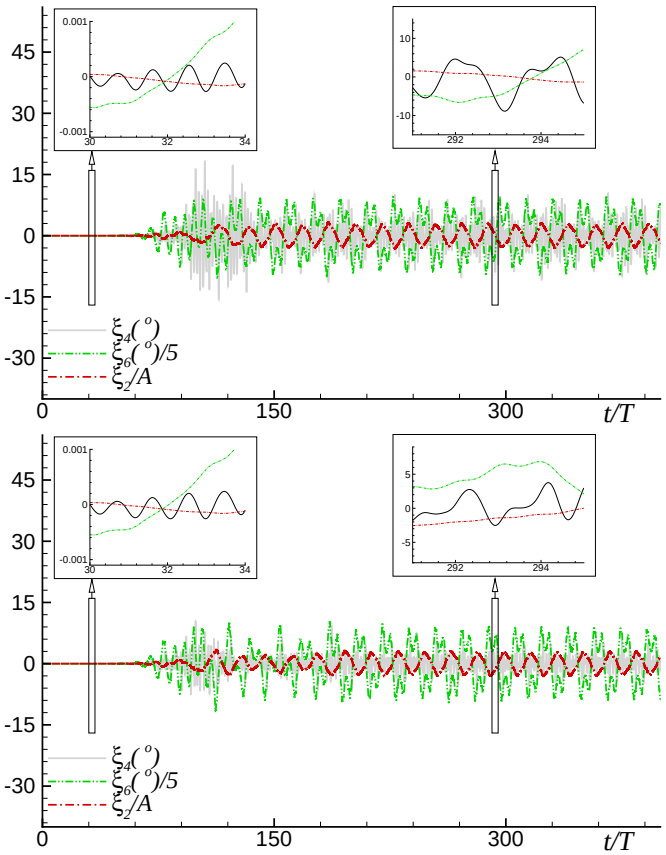

FIGURE 5. $\omega_{4n0}/\omega = 0.464$, $kA = 0.20$: NUMERICAL SWAY, ROLL AND YAW WITH MOORING-LINES, WITHOUT (TOP) AND WITH (BOTTOM) BILGE KEELS (l_{bk}/L=0.4 AND b_{bk}/B=0.03).

Steeper waves do not cause PR when sway and yaw are negligible (see enlarged view at smaller times in the top plot of figure 5). As these motions experience an unstable behavior with similar features as for kA=0.15 then the roll motion is also excited at its natural period tuning also in this case to $2T$ (see enlarged view at larger times in the same plot) but it is also evident the presence of the excitation period along the ξ_4 time history. One must note that the sway and yaw oscillation periods are different in the two wave-steepness cases. In particular, for kA=0.2 the yaw starts its unstable behavior with the same period as for kA=0.15 but, as the amplitude increases, the nonlinearities reduce its natural period and similarly it is predicted for the sway. The use of bilge keels has a similar effect as for the lower steepness; in this case the roll amplitude is kept below 9 degrees.

Figure 6 examines the maximum roll amplitude and the maximum amount of shipped water predicted without bilge keels for all examined cases with non negligible roll and with WOD. Here the maximum values are estimated along the whole examined time evolution, *i.e.* $t \leq 400T$, and one must note that they do not occur always periodically due to the chaotic behavior in many conditions. From the results, the roll amplitude can reach very high values and this is mainly due to nonlinear motion coupling, as discussed in [2]. In particular, the values are larger than the corresponding steady-state roll amplitudes predicted without mooring lines. For the largest incident-wave steepness there is almost a linear increase by decreasing the calm-water roll natural frequency-to-prescribed excitation frequency ratio. At $\omega_{4n0}/\omega = 0.464$, ξ_{4amax} is close to 20 degrees for almost all incident-wave steepnesses examined. For this frequency ratio, the parametric resonance occurs for all kA and is connected with influence of heave and pitch motions for the two lowest steepnesses and promoted by the coupling with sway and yaw for the others. When the bilge keels are introduced, there is a substantial reduction on the roll amplitude when the roll instability is connected with heave and pitch motions while the effect is more limited when the instability mechanism is due to the lateral motions. The roll amplitudes remain close to 10 degrees for $kA \geq 0.2$. This value is indicated by the horizontal dashed line in the figure and is often the maximum allowable roll amplitude for an FPSO in normal operational conditions. The maximum amount

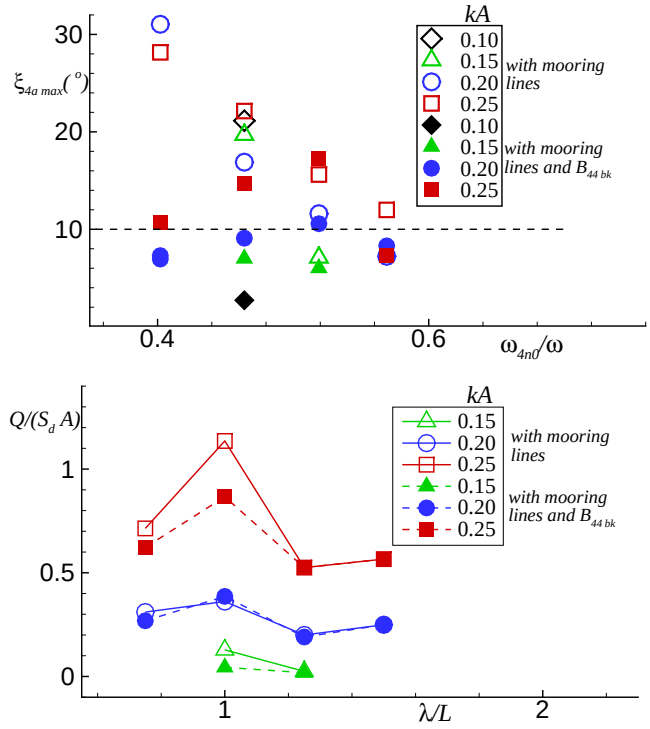

FIGURE 6. MAXIMUM NUMERICAL ROLL AMPLITUDE ξ_{4amax} (TOP) AND VOLUME OF SHIPPED WATER Q (BOTTOM), WITH MOORING LINES AND WITHOUT AND BILGE KEELS (l_{bk}/L=0.4 AND b_{bk}/B=0.03). S_d IS THE DECK AREA.

of shipped water is, in general, larger than without mooring lines when bilge-keels are not used and is less dependent on λ/L with local maxima at $\lambda/L = 1$. However, for the largest steepness, the bilge-keel effect on the WOD severity is very limited suggesting that the roll plays a minor role with respect to the other vertical motions which are not affected by the bilge-keel action in our model.

Table 6 examines the influence of the bilge-keel breadth and length on the roll for the case with largest ξ_{4amax} when l_{bk}/L=0.4 and b_{bk}/B=0.03 are assumed. Increasing b_{bk}/B to 0.04 has a

TABLE 6. $\omega_{4n0}/\omega = 0.519$, $kA = 0.25$: MAXIMUM NUMERICAL ROLL AMPLITUDE WITH MOORING-LINES, WITHOUT AND WITH BILGE-KEELS. DP= WITH A DYNAMIC-POSITIONING SYSTEM GIVING A LINEAR DAMPING IN ξ_1, ξ_2 AND ξ_6 EQUAL TO THE 15% OF THE CORRESPONDING CRITICAL DAMPING.

l_{bk}/L,b_{bk}/B	0,0	0.4,0.03	0.4,0.04	0.5,0.03	0.4,0.03,DP
xi_{4amax} (°)	15.6	17.3	16.0	15.5	3.9

very limited effect in this case and similarly it is obtained pushing the use of formula (1) beyond its applicability and so increasing l_{bk}/L to 0.5. This confirms the major role of the coupling with the horizontal motions, in particular sway and yaw, in the roll instability and suggests the need of a proper control for them to achieve an effective limitation of the roll amplitudes. Assuming a dynamic-positioning (DP) system, designed to provide a linear damping in surge, sway and yaw equal to the 15% of the corresponding critical damping, limits the roll amplitude below 4 degrees. This can be considered as a good damping level for a DP system used with FPSOs, in practice the level can be lower.

Figure 7 examines the effect of the bilge-keel damping for different heading angles assuming incident waves with $\omega_{4n0}/\omega = 0.464$ and, respectively, $kA = 0.1$ and $kA = 0.25$. The

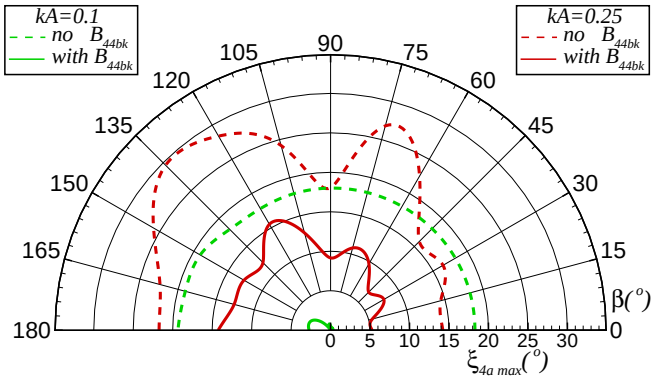

FIGURE 7. $\omega_{4n0}/\omega = 0.464$: POLAR DIAGRAM OF MAXIMUM ROLL AMPLITUDE IN WEATHER-VANING CONDITIONS, WITHOUT AND WITH BILGE KEELS (l_{bk}/L=0.4 AND b_{bk}/B=0.03).

maximum amplitude is predicted in weather-vaning conditions, *i.e.* after the FPSO has been rotated in yaw and brought to head-sea conditions by the mooring-lines. Without bilge-keels ξ_{4amax} is almost the same in all headings for the smalled steepenss. This is because the ship experiences parametric roll promoted by heave and pitch motions in waves and the responsible phenomena remain similar for the different cases once recovered head-sea conditions. For the largest steepness, the ship is subjected to roll instability due to coupling with lateral motions and the latter do not necessarily remain the same once recovered head-sea conditions if an instability has occurred for them. As for true head-sea conditions, the case with smallest steepness shows a suitable action of the bilge-keels in limiting the roll motion. For $kA = 0.25$, the bilge-keels are less effective, especially in bow and head-sea waves. In these conditions they are not able to limit the roll below 10 degrees.

For these two incident-wave scenarios, the effectiveness of the bilge-keels is documented in figure 8 in terms of maximum provided damping coefficient as a function of the heading angle. For the smallest steepness, an equivalent damping coeffi-

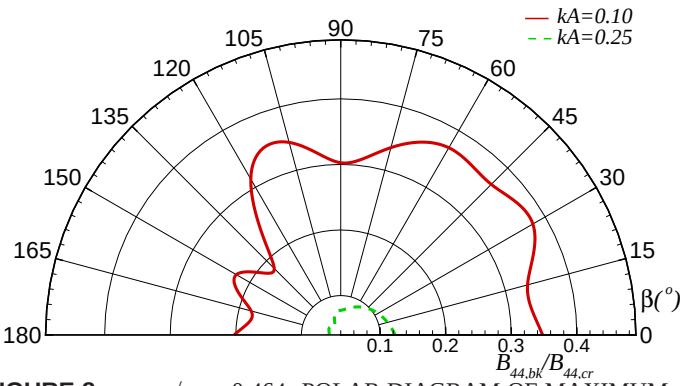

FIGURE 8. $\omega_{4n0}/\omega = 0.464$: POLAR DIAGRAM OF MAXIMUM BILGE-KEEL DAMPING COEFFICIENT B_{44bk} IN WEATHER-VANING CONDITIONS. B_{44cr} IS THE ROLL CRITICAL DAMPING.

cient slightly above the ten percent of the roll critical damping is needed to control the roll motion; for the largest *kA*, even a coefficient larger than the thirty percent of the critical damping is not enough to limit properly the roll.

SUMMARY

A 3D numerical Domain-Decomposition (DD) strategy for the seakeeping of a 6-dof ship with possible water-on-deck occurrence has been used to examine the effect of bilge keels on the stability of an FPSO without and with mooring lines. The seakeeping solver is based on the weak-scatterer hypothesis; water shipping is modelled as a 2D in-deck shallow water flow; the mooring lines are simulated within a quasi-static nonlinear approach and finally the bilge-keel damping is approximated using a simplified formula, best-fitting of the Ikeda's method. The performed analysis suggests that the bilge keels are well suited for the control of PR phenomena connected with large heave and pitch motions but are less effective in limiting the roll amplitude when sway-yaw-roll coupling involves instability phenomena. In the latter case it helps increasing the bilge-keel breadth or the length, but the latter parameter seems to play minor role in the considered range. The application of a suitable dynamic-positioning can compensate the limitations of bilge-keel action.

ACKNOWLEDGMENT

This research activity is partially funded by the Research Council of Norway through the Centres of Excellence funding scheme AMOS, project number 223254, and partially by the Flagship Project RITMARE - The Italian Research for the Sea - coordinated by the Italian National Research Council and funded by the Italian Ministry of Education, University and Research within the National Research Program 2011-2013.

The authors thank deeply Dr. Skjørdal for providing relevant practical information on FPSO arrangement.

REFERENCES

[1] Lugni, C., Greco, M., and O.M.Faltinsen, 2014. "Influence of yaw-roll coupling on the behavior of a FPSO: an experimental and numerical investigation". *Under review for Applied Ocean Research*.

[2] Greco, M., Lugni, C., and Faltinsen, O., 2015. "Influence of motion coupling and nonlinear effects on parametric roll for a FPSO". *in Phil. Trans. R. Soc. A.*, ***373***.

[3] Faltinsen, O. M., 2005. *Hydrodynamics of high-speed marine vehicles*. Cambridge University Press, Cambridge, UK.

[4] Neves, M., and Rodriguez, C., 2011. "On the assessment of parametric rolling of ships in head seas". In *Marine Technology and Engineering*, C. G. Soares, Y. Garbatov, N. Fonseca, and A. Teixeira, eds. pp. 563–573.

[5] Lee, J.-H., Kim, Y., and Song, K., 2014. "Simulation of parametric roll by using a semi-analytic approach". In Proc. of Int. Conference on Hydrodynamics (ICHD 2014).

[6] Greco, M., and Lugni, C., 2012. "3-d seakeeping analysis with water on deck and slamming. part 1: numerical solver". *Journal of Fluids and Structures*, ***33***.

[7] Pawlowski, J., 1991. "A theoretical and numerical model of ship motions in heavy seas". *SNAME Transactions*, ***99***, pp. 319–315.

[8] Rios, L. O. G., Bernitsas, M. M., and Nishimoto, K., 1997. Catenary mooring lines with nonlinear drag and touchdown. Tech. Rep. 333, Naval Architecture & Marine Engineering (SNAME).

[9] Kawahara, Y., Maekawa, K., and Ikeda, Y., 2011. "A simple prediction formula of roll damping of conventional cargo ships on the basis of Ikedas method and its limitation". In *Contemporary Ideas on Ship Stability and Capsizing in Waves*, M. Neves, V. Belenky, J. de Kat, K. Spyrou, and N. Umeda, eds., Vol. 97. pp. 465–486.

[10] de Oliveira, A., Fernandes, A. C., and Guimarães, H., 2012. "The influence of vortex formation on the damping of FPSOs with large width bilge keels". In Proceedings 31st International Conference Offshore Mechanics and Artic Engineering.

[11] Cummins, W., 1962. "The impulse response function and ship motions". *Symposium on Ship Theory, Schiffstechnik*, ***9***, pp. 101–109.

[12] Greco, M., , Lugni, C., and Faltinsen, O. M., 2014. "Can the water on deck influence the parametric roll of a FPSO? A numerical and experimental investigation". *European Journal of Mechanics - B/Fluids*, ***47***, pp. 188–201.